arXiv:cond-mat/0208364v1 [cond-mat.supr-con] 19 Aug 2002

$MgCNi_3$: Complex behavior in a strongly coupled superconductor

A. Wälte†, H. Rosner‡, M.D. Johannes‡, G. Fuchs† K.-H. Müller†, A. Handstein†, K. Nenkov†, V.N. Narozhnyi†, S.-L. Drechsler†, S. Shulga†, and L. Schultz†

† *Institut für Festkörper- und Werkstoffforschung Dresden, Postfach 270116, D-01171 Dresden, Germany*

and

‡*Department of Physics, University of California, Davis, California 95616*

(Dated: 1 August 2002)

Polycrystalline samples of the recently discovered $MgCNi_3$ superconductor were investigated by transport, ac susceptibility, dc magnetization and specific heat measurements in magnetic fields up to 16T. Consistent results were obtained for the temperature dependence of the upper critical field $H_{c2}(T)$ from resistance, ac susceptibility and specific heat measurements. A WHH like temperature dependence of $H_{c2}(T)$ and the quadratic relationship $H_{c2}(0) \sim T_c^2$ point to an effective predominant single band behavior near the quasi clean limit. Evidence for strong electron-phonon and electron-paramagnon coupling was found analyzing the specific heat data. The corresponding s- and p-wave scenarios are briefly discussed using calculated densities of states of different Fermi surface sheets.

PACS numbers: 74.70.Ad, 74.60.Ec, 74.60.Ge

Keywords: A. Superconductors, D. Upper critical field, Specific heat

I. INTRODUCTION

The recent discovery of superconductivity in the intermetallic antiperovskite compound $MgCNi_3$[1] with a superconducting transition temperature of $T_c \simeq 8$ K is rather surprising considering its high Ni content. Therefore, it is not unexpected that this compound is near a ferromagnetic instability which might be reached by hole doping at the Mg sites.[2] The possibility of unconventional superconductivity due to the proximity of these two types of collective order has attracted great interest in the electronic structure and the physics of the pairing mechanism. Band structure calculations[2,3,4] for $MgCNi_3$ reveal a domination of the electronic states at the Fermi surface by the 3d orbitals of Ni.

$MgCNi_3$ can be considered as the 3-dimensional analogue of the layered transition metal borocarbides which have superconducting transition temperatures up to $T_c \simeq 23$ K. In spite of the much lower T_c of $MgCNi_3$, its upper critical fields H_{c2} at low temperatures is, with $H_{c2}(0) = 10 \ldots 15$ T[5,6,7,8] comparable with that of the borocarbides or even higher. This is connected with the completely different temperature dependence of H_{c2} for these compounds. The $H_{c2}(T)$ dependence of $MgCNi_3$ is similar to that of dirty-limit intermetallic superconductors with a steep slope of $H_{c2}(T)$ at T_c.

Through analysis of specific heat data, $MgCNi_3$ was characterized in the framework of a conventional, phonon-mediated pairing both as a moderate[1,8] and as a strong[7] coupling superconductor. Strong coupling is also suggested by the large energy gap determined from tunneling experiments.[7] The question of the pairing symmetry is controversially discussed in the literature.[13]C NMR experiments[9] support s–wave pairing in $MgCNi_3$, whereas tunneling spectra indicate an unconventional pairing state.[7]

In the present investigation, upper critical field and specific heat data of $MgCNi_3$ were analyzed with the aid of theoretical results for Fermi velocities and partial densities of states in order to find out a consistent physical picture explaining the experimental results.

II. EXPERIMENTAL

Polycrystalline samples of $MgCNi_3$ have been prepared by solid state reaction. In order to obtain samples with high T_c, one has to use an excess of carbon as stated in Ref. 1. To cover the high volatility of Mg during the sintering of the samples an excess of Mg is needed, too.[1] In this study, a sample with the nominal formula $Mg_{1.2}C_{1.6}Ni_3$ has been investigated which is denoted as $MgC_{1.6}Ni_3$. To prepare the sample, a mixture of Mg, C and Ni powders was pressed into a pellet. The pellet was wrapped in a Ta foil and sealed in a quartz ampoule containing an Ar atmosphere at 180 mbar. The sample was sintered for half an hour at 600°C followed by one hour at 900°C. After a cooling process the sample was regrounded. This procedure was repeated two times in order to lower a possible impurity phase content. The obtained sample was investigated by x-ray diffractometry to estimate its quality. The diffractometer pattern (Fig. 1) showed small impurity concentrations mainly resulting from MgO and unreacted carbon crystallized in form of graphite. The lattice constant of the prepared sample was determined to be a = 0.38107(1) nm using the Rietveld computer program FULLPROF.[10] According to Ref. 11 this indicates that the nearly single phase sample corresponds to the superconducting modification of MgC_xNi_3.

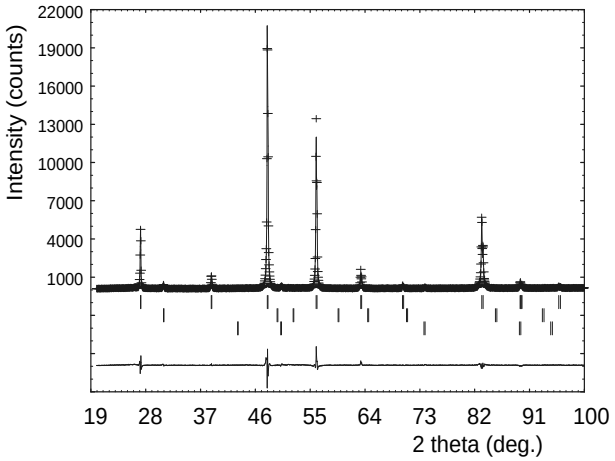


Figure 1: Rietveld refinement for $MgC_{1.6}Ni_3$. The crosses correspond to the experimental data. The solid line shows the calculated pattern. Vertical bars give the Bragg positions for the main phase $MgCNi_3$, graphite and MgO (from top to bottom). The line at the bottom gives the difference between the experimental and calculated data.

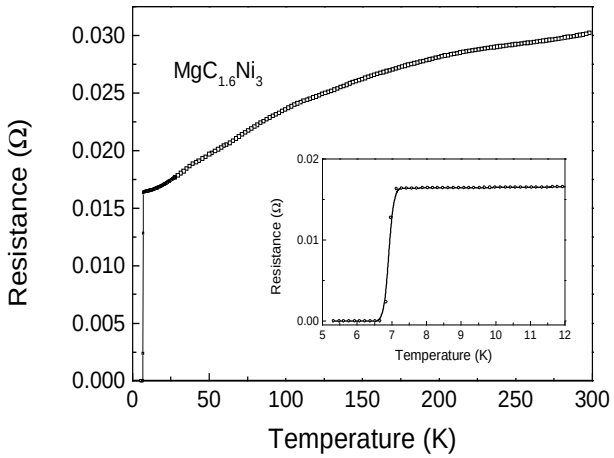


Figure 2: Temperature dependence of resistance of $MgC_{1.6}Ni_3$ at zero applied magnetic field. The inset shows the superconducting transition region.

The superconducting transition of the sample was investigated by measurements of the electrical resistance, the ac susceptibility and the specific heat. For the electrical resistance measurement a piece cut from the initially prepared pellet with 5mm in length and a cross section of approximately $1mm^2$ was measured in magnetic fields up to 16 T using the standard four probe method with current densities between 0.2 and 1 A/cm^2. The ac susceptibility and the specific heat measurements were performed on other pieces from the same pellet in magnetic fields up to 9 T.

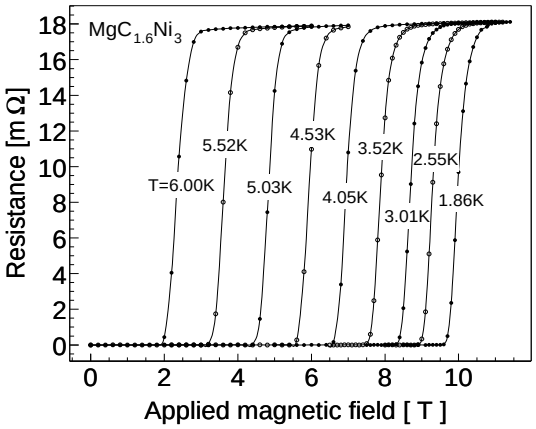


Figure 3: Field dependence of resistance of $MgC_{1.6}Ni_3$ measured at several temperatures.

III. RESULTS

A. Superconducting transition and upper critical field

In Fig. 2, the temperature dependence of the electrical resistance of the investigated sample is shown. A superconducting transition with an onset (midpoint) value of $T_c = 7.0$ K (6.9 K) is observed (see inset of Fig. 2) which is consistent with the onset of the superconducting transition at $T_c = 7.0$ K determined from ac susceptibility. It should be noted that the sample shown in Fig. 2 has a resistivity of $\rho_{300K} = 2.1$ mΩcm at 300 K which is much too large in order to be intrinsic. On the other hand, its residual resistance ratio $RRR = R(300K)/R(8K) = 1.85$ and the shape of the $R(T)$ curve are typical for $MgCNi_3$ samples.[1] A possible explanation for the high resistivity of the investigated sample which was not subjected to high pressure sintering is a relatively large resistance of the grain boundaries.

The field dependence of the electrical resistance of the same sample is shown in Fig. 3 for several temperatures between 6.0 and 1.9K. A sharp transition is observed which remains almost unchanged down to low temperatures. In Fig. 4, the fields H_{10}, H_{50} and H_{90} defined at 10%, 50% and 90% of the normal-state resistance are plotted as function of temperature. Identical results have been found from resistance–vs.–temperature transition curves measured at different magnetic fields. Additionally, Fig. 4 shows upper critical field data determined from ac susceptibility measurements. The onset of superconductivity was used to define H_{c2} from ac susceptibility.

It is clearly seen that for the investigated sample H_{c2}^{sus} (H_{c2} obtained from susceptibility) agrees approximately with H_{10}. A similar behavior was already observed for MgB_2, whereas in the case of rare–earth nickel borocarbides the onset of superconductivity determined from ac susceptibility was typically found to agree well with the

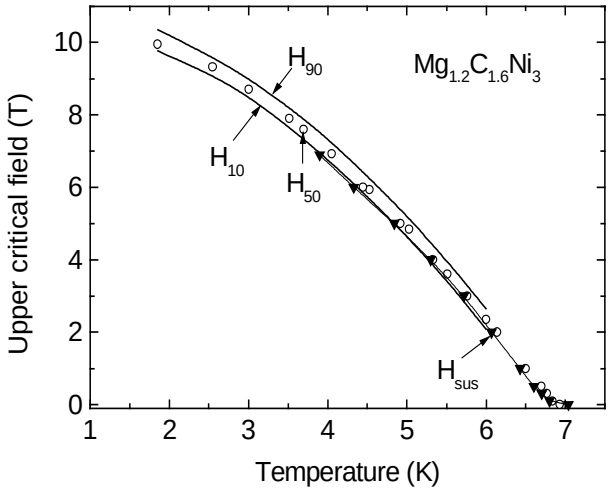


Figure 4: Temperature dependence of the upper critical field for $MgC_{1.6}Ni_3$. The circles show the midpoint value H_{50} of the resistivity in the normal state. The two lines labelled H_{10} and H_{90} denote 10% and 90% of the normal state resistivity. The triangles represent the upper critical field determined from the onset of ac susceptibility.

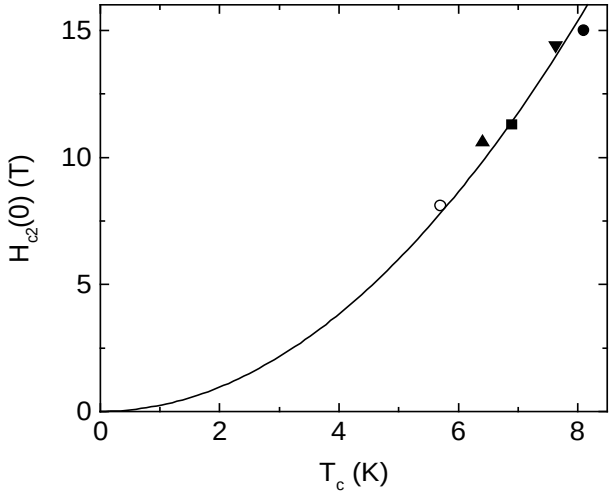


Figure 5: Upper critical field at zero temperature vs. superconducting transition temperature for the $MgC_{1.6}Ni_3$ sample of this work (■) and of several $MgCNi_3$ samples reported in Ref. 3 (◯), Ref. 4 (•), Ref. 5 (▼) and Ref. 6 (▲). The experimental data can be described by a quadratic law (solid line).

midpoint value (H_{50}) of the normal state resistivity. The width $\Delta H = H_{90} - H_{10}$ of the superconducting transition curves in Fig. 3 (and Fig. 4) remains, with $\Delta H \simeq 0.6$ T, almost unchanged down to low temperatures. A polycrystalline sample of a strongly anisotropic superconductor shows a gradual broadening of the superconducting transition with decreasing temperature as was observed, for example, for MgB_2.[12] Therefore, the nearly constant transition width ΔH observed for the investigated sample can be considered as an indication of a rather small anisotropy of $H_{c2}(T)$ in $MgCNi_3$.

The extrapolation of $H_{90}(T)$ to $T = 0$ yields an upper critical field of $H_{c2}(0) \simeq 11.3$ T. The observed temperature dependence of the upper critical field is typical for $H_{c2}(T)$ data reported for $MgCNi_3$ and was described[6,7,8] within the standard WHH model[13] by conventional superconductivity in the dirty limit. The WHH model predicts a relation $H_{c2}(0) \propto (-dH_{c2}/dT)_{T=T_c} \cdot T_c$. Available data for $MgCNi_3$, including those presented in this paper show a strong variation of $H_{c2}(0)$ with T_c (see Fig. 5), whereas $(dH_{c2}/dT)_{T_c} \approx -(2.65 \pm 0.2)$ T/K remains almost unchanged. Considering the data in Fig. 5, the linear dependence of $H_{c2}(0)$ on T_c predicted for constant $(dH_{c2}/dT)_{T_c}$ by the WHH model can be ruled out.

The solid line in Fig. 5 corresponds to a quadratic law $H_{c2}(0) \sim T_c^2$ which is the benchmark for the clean limit. Indeed in the isotropic single band s–wave clean limit one has[14]

$$H_{c2}(0)\,[\mathrm{Tesla}] = 0.0237 \frac{(1+\lambda)^{2.2}\, T_c^2\,[\mathrm{K}]}{v_F^2\,[10^5 \frac{\mathrm{m}}{\mathrm{s}}]} \qquad (1)$$

Compared with WHH the effect of strong coupling (measured by the dimensionless electron-phonon coupling constant λ) is an enhancement of H_{c2} primarily through the renormalization of the bare Fermi velocity $v_F \rightarrow v_F/(1+\lambda)$ and a weak enhancement factor coming from the energy dependence of the gap function. The strong coupling ($\lambda \approx 3.4$ near the Brillouin zone boundary and zero at the zone center) to the rotational mode near 13 meV proposed in Ref. 3 gives an upper limit for a strong coupling required to reproduce upper critical fields as high as $12 \ldots 15$ T. Using the averaged Fermi velocities of $1.45 \cdot 10^5$ m/s for the rounded cube–like Fermi surface shown in Fig. 11 we arrive at $\lambda \approx 2.5 \ldots 3$.

B. Specific heat

Specific heat measurements were performed in order to get additional information about $H_{c2}(T)$, the superconducting pairing symmetry and the strength of the electron–phonon coupling from thermodynamic data. In Fig. 6 specific heat data, c_p/T vs. T^2, are shown for applied magnetic fields up to 8T. The upper critical fields, $H_{c2}(T)$, determined from the specific heat data, are shown in Fig. 7. It is clearly seen that the $H_{c2}(T)$ data obtained from the specific heat are located in the small field range between the $H_{90}(T)$ and $H_{10}(T)$ curves.

In order to describe the experimental data of the normal state specific heat in zero field between T_c and $30K$ (see Fig. 8) the expression

$$c_n(T) = \gamma_N T + c_{\mathrm{lattice}} + c_{\mathrm{Einstein}} + n c_{\mathrm{Schottky}} \qquad (2)$$

was used. The linear–in–T term is due to the electronic contribution with γ_N as the Sommerfeld parameter. The

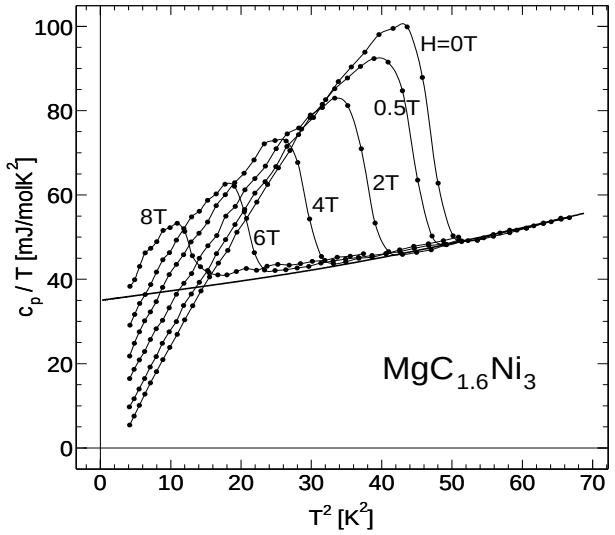


Figure 6: Specific heat data c_p/T vs. T^2 of $MgC_{1.6}Ni_3$ measured at various magnetic fields up to 8T. The solid line is a fit of Eq.(2) to the data for $H = 0$ above T_c. Its intersection with the ordinate gives the Sommerfeld parameter γ_N.

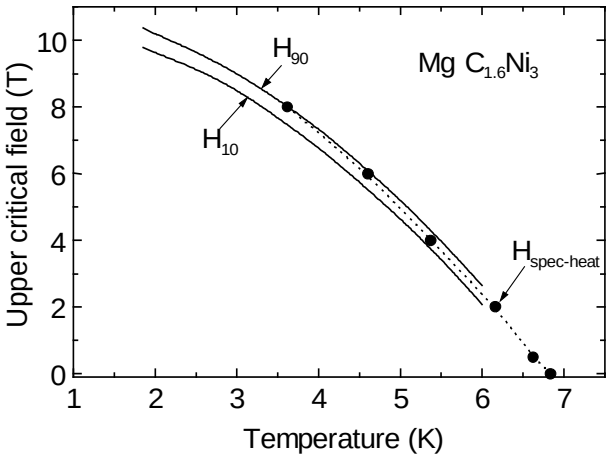


Figure 7: Comparison of upper critical field data determined from specific heat (•) and resistance measurements for $MgC_{1.6}Ni_3$. H_{10} and H_{90} were determined at 10% and 90% of the normal state resistivity, respectively. An entropy conserving construction was used to determine the upper critical field from the specific heat data of Fig. 6.

second term, $c_{lattice} = \beta T^3 + \delta T^5$ represents the phonon contribution. This extension of the usual Debye approximation $c_{lattice} \propto T^3$ includes deviations from the linear dispersion of the acoustic modes and is required in order to describe the phonon contribution to the specific heat in an extended temperature range. The same procedure has already been used to describe the specific heat of MgB_2.[15] An additional single Einstein mode, $c_{Einstein}$, was used to take into account the contribution of the previously mentioned lowest energy optical mode near 13meV.[3] The last part, $nc_{Schottky}$, represents the contribution of a conventional two-level Schottky model which was used to describe the slight upturn of the specific heat just above the superconducting transition temperature T_c (see Fig. 8). This feature possibly results from contributions of paramagnetic impurities like unreacted Ni (the prefactor n gives the concentration of these impurities).

The fitting procedure returned a Sommerfeld parameter $\gamma_N = 35 mJ/molK^2$ which is close to the reported values of $\gamma_N = 27.6$[7] and $33 mJ/molK^2$.[8] The Debye temperature was found to be $\Theta_D = 289K$ and the energy of the optical phonon mode resulting from the fit is 9.5meV which slightly deviates from the theoretically proposed value (13meV).[3] The paramagnetic impurity concentration derived from the fit is $n \approx 4.5\%$ and the energy gap of the Schottky anomaly is 5.3meV. As shown in Fig. 8, the experimental data are very well described by Eq. (2) in the investigated temperature range $T_c < T < 30K$. The jump Δc of the specific heat at T_c (see inset of Fig. 8) is given by the difference between the experimental data, c_p and the normal specific heat contribution, c_n.

The transition temperature $T_c = 6.83K$ obtained from the inset of Fig. 8 agrees approximately with the transition temperatures $T_c = 7.0K$ and $T_c = 6.9K$ derived from ac susceptibility and from resistance data, respectively. In the low temperature region the experimental data for $\Delta c/T$ versus T can be described by the BCS–like expression

$$\Delta c = 7.95 \gamma_N T_c \exp\left(-\frac{\Delta(0)}{k_B T}\right) - \gamma_N T \qquad (3)$$

using $2\Delta(0)/k_B T_c = 2.96$ instead of $2\Delta_{BCS}(0)/k_B T_c = 3.52$ predicted by the BCS model. Above $T = 4K$ the fit of Eq. (3) starts to deviate from the experimental curve resulting in a much lower value for the jump at $T = T_c$ than observed experimentally. Notice that the experimental value of the jump, $\Delta c/\gamma_N T_c = 1.6$, nearly corresponds to the BCS value $\Delta c/\gamma_N T_c = 1.43$ indicating weak electron–phonon coupling. This contrasts to the strong coupling derived from Eq. (1) and $H_{c2}(0)$ data. A natural explanation for this discrepancy is the two–band character of $MgCNi_3$ which will be discussed in the next section.

To examine the temperature dependence of the electronic specific heat

$$c_{el}(T) = \Delta c + \gamma_N T \qquad (4)$$

at $H = 0$ in detail, $c_{el}(T)/\gamma_N T_c$ is plotted logarithmically vs. T_c/T in Fig. 9. It is clearly seen, that the experimental data at low temperatures ($T_c/T > 2$) follow the modified BCS expression (Eq. (3), solid line). We found that this exponential law is not affected by the low temperature branch of the Schottky term in Eq. (2) which has an exponential temperature dependence, too. The exponential temperature behavior of the electronic specific heat at low temperatures found for $MgCNi_3$ is a strong indication for s–wave superconductivity in this compound.

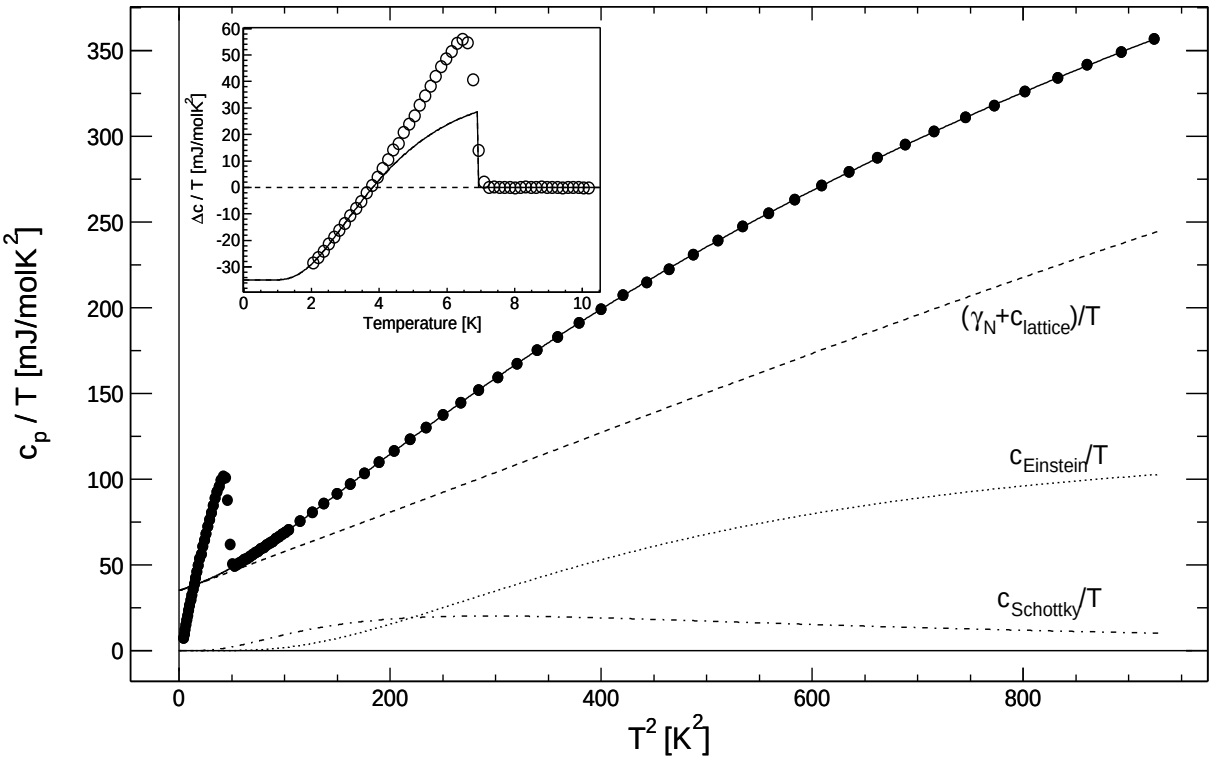


Figure 8: Specific heat data c_p/T vs. T^2 of $MgC_{1.6}Ni_3$ at zero magnetic field. According to Eq.(2), the dashed line represents the lattice contribution, the dotted line shows the contribution from a rotational phonon mode (see text) and the dash-dotted line gives a Schottky contribution. Inset: Contribution of the superconducting electrons to the specific heat $\Delta c/T = (c_p - c_n)/T$. The solid line in the inset is a fit of the BCS expression to the data with parameters according to Eq. (3). The conservation of entropy was confirmed by integrating of $\Delta c/T$ in the temperature range $0 < T < T_c$ (according to the data above 2K and the solid line below 2K).

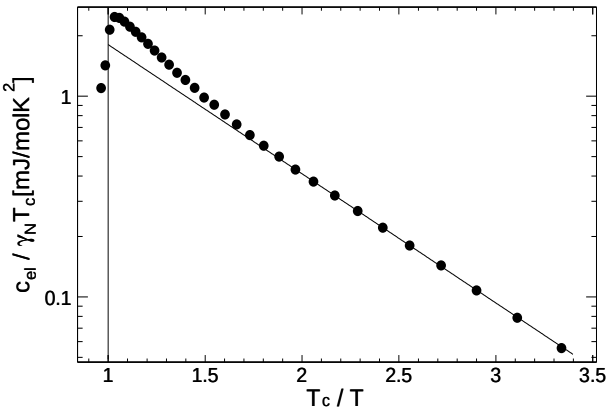


Figure 9: Normalized electronic specific heat contribution of $MgC_{1.6}Ni_3$ vs. T_c/T. The comparison of the data with the BCS expression (solid line) corresponding to Eq. (3) clearly shows the exponential temperature dependence of the electronic specific heat at low temperatures.

In the superconducting state, a linear–in–T electronic specific heat contribution $\gamma(H)T$ arises from the normal conducting cores of the flux lines for applied magnetic fields $H > H_{c1}$. This contribution can be expressed as $\gamma(H)T = c_p(T,H) - c_p(T,0)$,[16] where $c_p(T,0)$ is the specific heat in the Meissner state. Specific heat data for $MgC_{1.6}Ni_3$ at $T = 2$K (see inset of Fig. 10) were analyzed in order to derive the field dependence of $\gamma(H)$. In Fig. 10, the obtained $\gamma(H)/\gamma_N$ is plotted against $H/H_{c2}(0)$ using the Sommerfeld parameter $\gamma_N = 35$mJ/molK^2 and $H_{c2}(0) = 11.3$T. Not shown in this plot are high-field data which are influenced by an additional contribution to the specific heat in the normal state arising in magnetic fields. This contribution which is clearly seen in Fig. 6 as deviation of the c_p/T data from the solid line causes a shift of the high-field c_p/T data in the superconducting state to higher values. The origin of this effect is not yet understood. Its influence on the field dependence of c_p/T at $T = 2$K is illustrated in the inset of Fig. 10. At low magnetic fields, a negative curvature is observed which starts to change its sign at fields above 4T.

The low-field data of c_p/T shown in Fig. 10 can be described by the expression $\gamma/\gamma_N = (H/H_{c2}(0))^{0.6}$ which differs from the linear $\gamma(H)$ law expected for isotropic s-wave superconductors in the dirty limit. A non-linear field dependence close to $\gamma(H) \propto H^{0.5}$ has been reported for some unconventional superconductors with gap nodes in the quasiparticle spectrum of the vortex state as in $YBa_2Cu_3O_7$,[17] and in the heavy fermion superconduc-

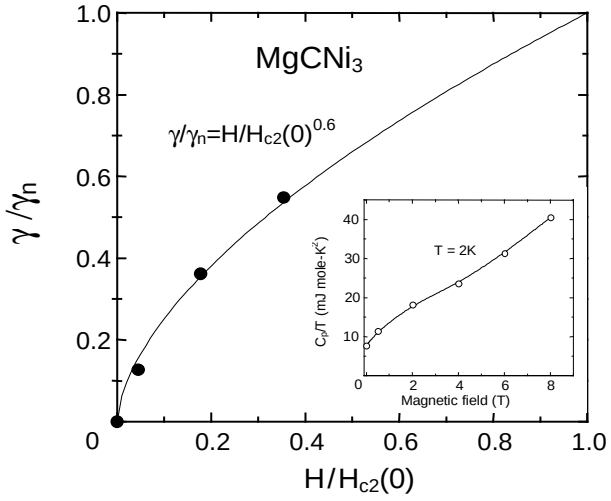


Figure 10: Field dependence of the specific heat contribution $\gamma(H)$ of the vortex core electrons in the mixed state normalized by the Sommerfeld parameter $\gamma_{\rm N}$ and $H_{\rm c2}(0)$. The black line is a fit of $\gamma(H)/\gamma_{\rm N} = (H/H_{\rm c2}(0))^{0.6}$ to the experimental data. Inset: Field dependence of the specific heat $c_{\rm p}/T$ at $T = 2$K.

tor UPt_3,[18] but also in some clean s-wave superconductors such as $CeRu_2$,[19] $NbSe_2$[16,20] and the borocarbides RNi_2B_2C (R = Y, Lu).[21,22] Delocalized quasiparticle states around the vortex cores, similar to these in d-wave superconductors, seem to be responsible for the non–linear $\gamma(H)$ dependence in the borocarbides.[23,24]

IV. DISCUSSION

In principle, the upper critical field data found for $MgCNi_3$ could be understood both in the s- and p-wave scenario. The high magnitude of the upper critical fields might be achieved in s-wave superconductors, but also in a clean limit weak coupling p-wave case employing the "slow" holes on the "four-leafed clover"–like Fermi surface sheets with $0.5 \cdot 10^5$m/s (see Fig. 11). Following Maki et al.[25] an additional numerical factor 1.3 should be introduced in this case in Eq. (1). The different temperature dependence of the electronic specific heat at low temperatures in *s*- and *p*-wave superconductors allows the discrimination between predominant s- and p-wave scenarios. As mentioned above, the exponential temperature behavior of the electronic specific heat found for $MgCNi_3$ is a strong indication for *s*-wave superconductivity in this compound.

It is convenient to rewrite Eq. (1) using experimentally accessible quantities as the plasma energy $\omega_{\rm pl}$, the volume of the unit cell V, and the Sommerfeld constant γ_N. Then, Eq. (5) provides a criterion for a superconductor which can be described in the clean limit within the isotropic single band model:

$$Q = \frac{3.6\omega_{\rm pl}^2\,[{\rm eV}^2]\,H_{\rm c2}(0)\,[{\rm T}^2]\,V\left[\left(10^{-10}m\right)^3\right]}{\gamma_{\rm N}\,[{\rm mJ/molK}^2]\,T_{\rm c}^2\,[{\rm K}]\,(1+\lambda)^{1.4}} \qquad (5)$$

If Q differs significantly from 1, a more complex model should be considered.

Some values for Q are summarized in Tab. I.

	$\omega_{\rm pl}$	$H_{\rm c2}(0)$	V	$\gamma_{\rm N}$	$T_{\rm c}$	λ	Q
Nb	9.9	0.35	18	7.8	9.3	0.9	1.4
YNi_2B_2C	4.0	10	64	19	15	0.7	4.1
MgB_2	7.0	17	29	3.0	40	0.8	7.9
MgB_2	7.0	17	29	3.0	40	2.5	3.1
$MgCNi_3$	3.2	15	56	35	8	1.0	5.2
$MgCNi_3$	3.2	15	56	35	8	2.5	2.4

Table I: Values of Q and further parameters (see text) for selected superconductors. Q is a measure for the applicability of the isotropic single band model. A deviation from $Q \approx 1$ indicates the need for a more complex model. For MgB_2 and $MgCNi_3$, two limiting values for λ are consiered for illustration.

The crystal structure of $MgCNi_3$ can be seen as a three dimensional analogue of the layered borocarbides. Thus it is instructive to compare the results with the electronic specific heat dependence of the borocarbides and the boronitrides which were found to be isostructural to the borocarbides. The electronic specific heat of $La_3Ni_2B_2N_{3-\delta}$ exhibits an exponential temperature dependence[26] as does $MgCNi_3$, while that of YNi_2B_2C or $LuNi_2B_2C$ follows a power law of the type $c_{\rm el} = 3\gamma_{\rm N}\left(\frac{\rm T}{\rm T_c}\right)^{\rm a}$ with an exponent $a \approx 3$.[27,28]

The electron-phonon coupling constant λ in $MgCNi_3$ averaged over all Fermi surface sheets can be estimated from the relation

$$\gamma_{\rm N} = \frac{\pi^2}{3}k_{\rm B}^2\,(1+\lambda)\,N(E_{\rm F}) = \gamma_0\,(1+\lambda) \qquad (6)$$

using the experimental value of the Sommerfeld constant $\gamma_{\rm N} = 35{\rm mJ/molK}^2$ and the density of states (DOS) at the Fermi level $N(E_{\rm F})$ calculated within the local density approximation. From the calculated density of states and the corresponding bare specific heat coefficient, $\gamma_0 = 11{\rm mJ/molK}^2$ one obtains a large electron-phonon coupling constant $\lambda = 2.2$.

According to band structure calculations using the full-potential nonorthogonal local-orbital minimum-basis scheme[29] within the local density approximation, the total DOS can be decomposed into a roughly 15% and a 85% contribution stemming from the fast and the slow sheets of the Fermi surface, respectively. Then, the total

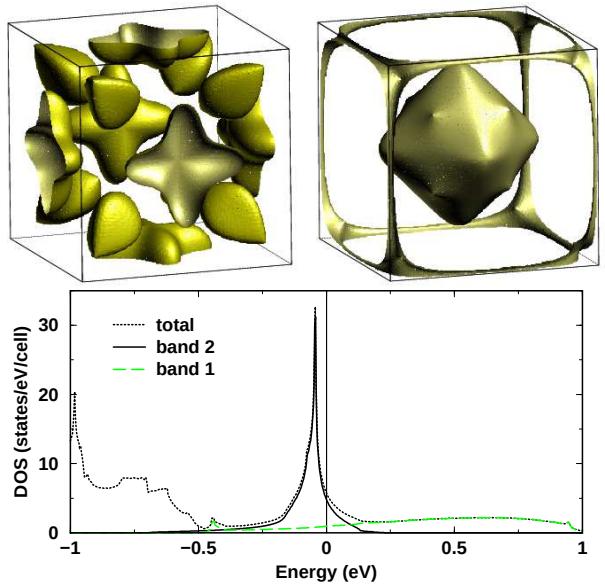


Figure 11: The two Fermi surface sheets of $MgCNi_3$ and the corresponding band resolved density of states near the Fermi level. "Band 1" corresponds to the Fermi surface sheet in the topright panel, "band 2" to the Fermi surface in the topleft panel.

coupling constant averaged over all Fermi surface sheets reads

$$\lambda_{\rm tot} = \lambda_1 \frac{\rm N_1(0)}{\rm N(0)} + \lambda_2 \frac{\rm N_2(0)}{\rm N(0)} \qquad (7)$$

and with the aid of $\lambda_{\rm tot} = 2.2$ and $\lambda_1 \approx 2.5 \ldots 3$ estimated from the upper critical field $H_{c2}(0) \approx 12 \ldots 15$T, respectively (Eq. (1)) one arrives at $\lambda_2 \approx 2.0 \ldots 2.1$. The question then arises about the origin of these strong mass enhancements in both bands. Obviously λ_2 cannot be of electron-phonon nature alone, since otherwise one should ask, why are T_c, the above mentioned gap, and $H_{c2}(0)$ so low? So we are forced to assume that λ_2 should be decomposed into an electron-phonon contribution and a pair-breaking electron-paramagnon λ_{sf} (electron-spin fluctuation) one. We adopt for the electron-phonon part a typical transition metal value, say $\lambda_{2ph} \sim 1$. From Fig. 11, a band width of about 0.6 eV can be estimated for band 2. Taking the average of the electron and the hole Fermi energies as a representative effective Fermi energy of band 2 $\hbar\omega_{2F} \approx 0.3$ eV can be estimated. Then, according to the Berk-Schrieffer theory the paramagnon spectral density should exhibit a maximum near $\hbar\omega_{sf} \approx \hbar\omega_{2F}/S \sim$ 80 meV, where $S \approx 4$ is the Stoner factor. Since this frequency exceeds considerably the typical phonon frequencies, the effect of the paramagnon pair breaking is somewhat reduced due to the pseudopotential effect[30], well-known for the large bare Coulomb repulsion μ where it produces the smaller pseudopotential μ^*-value due to the large logarithmic factor of about 5 entering its denominator. In the present case, this factor is reduced to 1.4, only. Then the "bare" paramagnon coupling constant $\lambda_{sf} \sim 1$ is reduced to about $\lambda^*_{sf} \sim 0.4$. Together with standard Coulomb pseudopotential, e.g. 0.13, one nevertheless arrives at a sizable suppressed pairing in band 2 which is responsible for the observed small gap seen in the low T specific heat data. The missing od only very weakly pronounced curvature in $H_{c2}(T)$ near T_c points to weak interband coupling, a posteriori justifying our one band estimate for $H_{c2}(0)$ given above. A more quantitative study must await more detailed knowledge on the phonon and paramagnon spectra.

V. CONCLUSION

The electronic specific heat shows an exponential temperature dependence at low temperatures which is a strong indication for s-wave pairing symmetry in this compound. Strong electron-phonon coupling has been derived from specific heat data and the calculated densitiy of states averaged over all Fermi surface sheets. Comparing $MgCNi_3$ with other multi-band superconductors such as MgB_2 or transition metal borocarbides, one concludes that the disjoint Fermi surface sheets differ from each other not only in the strength of the electron-phonon interaction or the Fermi velocities but to the best of our knowledge also in strength of the depairing interaction. Approaching the remarkable peak in the DOS slightly below the Fermi energy, an interesting enhancement of the paramagnon contribution followed by a gapless Fermi surface sheet and a possible p-wave superconductivity mediated by ferromagnetic spin fluctuations might be expected. In any case, the competing interplay of strong electron-phonon and electron-paramagnon interactions together with a strongly energy dependent DOS on disjoint, almost decoupled Fermi surface sheets is a great challenge for future theoretical and experimental work.

Acknowledgments

The Sonderforschungsbereich 463 at the TU Dresden, the DAAD (H.R.), the NSF (DMR-0114818) and the DFG are gratefully acknowledged for financial support. We thank T. Mishonov for discussions.

[1] T. He, Q. Huang, A. P. Ramirez, Y. Wang, K. A. Regan, N. Rogado, M. A. Hayward, M. K. Haas, J. S. Slusky, K. Inumara, et al., Nature **411**, 54 (2001).

[2] H. Rosner, R. Weht, M. D. Johannes, W. E. Pickett, and E. Tosatti, Phys. Rev. Lett. **88**, 027001 (2002).

[3] D. J. Singh and I. Mazin, cond-mat/0105577.

[4] S. B. Dugdale and T. Jarlborg, Phys. Rev. B **64**, 100508 (2001).

[5] S. Y. Li et al., cond-mat/0104554.

[6] S. Y. Li, R. Fan, X. H. Chen, C. H. Wang, W. Q. Mo, K. Q. Ruan, Y. M. Xiong, X. G. Luo, H. T. Zhang, L. Li, et al., Phys. Rev. B **64**, 132505 (2001).

[7] Z. Q. Mao, M. M. Rosario, K. D. Nelson, K. Wu, I. G. Deac, P. Schiffer, and Y. Liu, cond-mat/0105280(v3).

[8] J.-Y. Lin, P. L. Ho, H. L. Huang, P. H. Lin, Y.-L. Zhang, R.-C. Yu, C.-Q. Jin, and H. D. Yang, cond-mat/0202034.

[9] P. M. Singer, T. Imai, T. He, M. A. Hayward, and R. J. Cava, Phys. Rev. Lett. **87**, 257601 (2001).

[10] Rietveld refinement program FULLPROF 2k.

[11] Z. A. Ren, G. C. Che, S. L. Jia, H. Chen, Y. M. Ni, G. D. Liu, and Z. X. Zhao, Physica C **371**, 1 (2002).

[12] G. Fuchs, K.-H. Müller, A. Handstein, K. Nenkov, V. N. Narozhnyi, D. Eckert, M. Wolf, and L. Schultz, Sol. State Comm. **118**, 497 (2001).

[13] N. R. Werthammer, E. Helfand, and P. C. Hohenberg, Phys. Rev. **147**, 295 (1966).

[14] S. V. Shulga and S.-L. Drechsler, cond-mat/0202172. A linear fit yields a negative interception in contradiction with the expected behavior in the dirty limit case. If one would adopt nevertheless a dirty limit scenario, the measured (reported in Ref. Cava residual resistivity of $\rho(8\mathrm{K}) = 1.14$ mΩcm (40 mΩcm) corresponds to an upper critical field of the order of about 5000 (250) Tesla, where a plasma frequency of 3.25 eV 11 and our calculated averaged Fermi velocity of $1.45{\cdot}10^5$ m/s have been adopted. Thus we conclude that the reported so far resistivity data do not reflect the intrinsic properties of polycrystalline grains.

[15] C. Wälti, E. Felder, C. Degen, G. Wigger, R. Monnier, B. Delley, and H. R. Ott, Phys. Rev. B **01**, 172515 (2001).

[16] J. E. Sonier, M. F. Hundley, J. D. Thompson, and J. W. Brill, Phys. Rev. Lett. **82**, 4914 (1998).

[17] D. A. Wright, J. P. Emerson, B. F. Woodfield, J. E. Gordon, R. A. Fisher, and N. E. Phillips, Phys. Rev. Lett. **82**, 1550 (1999).

[18] A. P. Ramirez, N. Stücheli, and E. Bucher, Phys. Rev. Lett. **74**, 1218 (1995).

[19] M. Hedo, J. Phys. Soc. Japan **67**, 272 (1998).

[20] M. Nohara, M. I. F. Sakai, and H. Takagi, J. Phys. Soc. Japan **68**, 1078 (1999).

[21] M. Nohara, M. Isshiki, H. Takagi, and R. J. Cava, J. Phys. Soc. Japan **66**, 1888 (1997).

[22] D. Lipp, M. Schneider, A. Gladun, S.-L. Drechsler, J. Freudenberger, G. Fuchs, K. Nenkov, K.-H. Müller, T. Cichorek, and P. Gegenwart, Europhys. Lett. **58**, 435 (2002).

[23] K. Izawa, A. Shibata, Y. Matsuda, Y. Kato, H. Takeya, K. Hirata, C. J. van der Beek, and M. Konczykowski, Phys. Rev. Lett. **86**, 1327 (2001).

[24] E. Boaknin, R. W. Hill, C. Proust, C. Lupien, L. Taillefer, and P. C. Canfield, Phys. Rev. Lett. **87**, 237001 (2001).

[25] K. Maki, E. Puchkarev, and G. F. Wang, *High-T_c superconductors and related Materials*, Series 3 High Technology v. 86, (Ed. S.-L. Drechsler and T. Mishonov), (Kluwer Academic Publisher Dordrecht, 2001).

[26] H. Michor, R. Krendelsberger, G. Hilscher, E. Bauer, C.Dusek, R. Hauser, L. Naber, D. Werner, P. Rogl, and H. W. Zanbergen, Phys. Rev. B **54**, 9408 (1996).

[27] H. Michor, T. Holubar, C. Dusek, and G. Hilscher, Phys. Rev. B **52**, 16165 (1995).

[28] N. M. Hong et al., Physica C **227**, 85 (1994).

[29] K Koepernik and H. Eschrig, Phys. Rev. B **59**, 1743 (1999). For details of the calculations see Ref. 2.

[30] A. P. Zhernov and S. L. Drechsler, Fizika Nizkikh Temperatur (Sov. Low Temp. Phys.) **11**, 899 (495) (1985).